Available online at www.sciencedirect.com
ScienceDirect
Journal of the European Ceramic Society 27 (2007) 1435–1441
www.elsevier.com/locate/jeurceramsoc

Structure of kaoline–alumina based foam ceramics for high temperature applications

Thomas Juettner [a,*], Heinrich Moertel [a], V. Svinka [b], R. Svinka [b]

[a] *University Erlangen-Nuremberg, Department of Materials Science and Engineering, Institute III Glass and Ceramics, Martensstr. 5, D-91058 Erlangen, Germany*
[b] *RTU Institute of Silicate Materials, Technical University Riga, Azenes Str. 14/24, Riga LV 1048, Latvia*

Available online 22 May 2006

Abstract

Light weight refractory materials were developed applying the aerated concrete technology. Kaolinite based suspensions were agitated with Al powders or Al pastes. Under release of hydrogen gas, foams were formed at pH values from 7 to 9, stabilised, dried and fired at temperatures up to 1600 °C. Loading fractions of alumina up to 80 vol.% were demonstrated. The porosity varies with the amount of the metal precursor Al. A macro porosity of 0.2–1 mm was formed which was characterised by image analysis and X-ray tomography. The working temperature of the produced refractory materials depends on the prefiring temperature, the filler character and content and the macroscopic structure. Silica free pure porous mullite or mullite-corundum ceramics were obtained. Thermal analysis shows that the porous refractories meet the ASTM requirements for application temperatures up to 1550 °C.

Keywords: Slip casting; Porosity; X-ray methods; Mullite; Refractories

1. Introduction

There is a large demand for economic and ecologic solutions for porous light weight materials with high temperature applications in the ceramics industry. Those light weight bricks are usually based on mullite and alumina and were produced by burning out organic matter.[1–3] Former investigations have shown that lightweight materials can be produced according to the aerated concrete technology with metal powders or pastes based on Al serving as pore foaming agent.[4,5]

Mullite, the only stable binary crystalline phase in the SiO_2–Al_2O_3 system may be produced by thermal decomposition of aluminosilicates.[6–8] Due to its excellent properties mullite is an important material for high temperature engineering and high temperature structural applications.[9,10] Polycrystalline mullite has a lower thermal expansion coefficient in the temperature range from 25 to 800 °C than alumina ($\alpha = 5 \times 10^{-6}$ 1/K), giving rise to an excellent thermal shock resistance.[11] Starting materials for producing porous mullite ceramics are kaolinite powders or pellets. The reaction series of kaolinite or metakaolinite yields mullite. Initially the transient alumina type spinel starts to form at a temperature of 980 °C (exothermic effect),[12,13] and mullite crystallisation follows at higher temperatures.[14] Kaolinites have a two layer structure with molecular sheets of $(Si_2O_5)^{2-}$ and $[Al_2(OH)_4]^{2+}$. Si^{4+} and Al^{3+} are not sufficient mixed in kaolinite to prevent the segregation of alumina and amorphous silica, which may crystallise as cristobalite at high temperatures. Sintering of kaolinite and alumina mixtures can yield mullite–alumina functionally gradient ceramics.[15] The aim of this study was to produce light weight refractory material using a technology adapted from the aerated concrete technology to reduce emissions from burning out organic matter and to produce a more uniform pore structure for applications in industry.

2. Experimental procedure

Table 1 shows the properties of the used raw materials. Kaolin Zettlitz Premier (Czech Republic) together with alumina (Russia) was dry mixed an then suspended in water (water content 33 wt.%).

Different amounts (0.03, 0.05, 0.08, 0.10, 0.15 wt.%), starting with 0.03 wt.%, of Al paste (Schlenk Metallpulver GmbH, Roth-Barnsdorf, Germany) were added and then the suspension

* Corresponding author. Tel.: +49 9131 85 27564; fax: +49 9131 85 28311.
E-mail addresses: thomas.juettner@ww.uni-erlangen.de (T. Juettner), svinka@ktf.rtu.lv (V. Svinka).

0955-2219/$ – see front matter © 2006 Elsevier Ltd. All rights reserved.
doi:10.1016/j.jeurceramsoc.2006.04.029

Table 1
Characteristic data of used materials

	Kaoline	Alumina	Aluminium paste
Density (g/cm^3)	2.62	4.0	2.7
d_{50} particle size (μm)	3.5	90	15
Spec. surface (m^2/g)	16	60	–
Loss on ignition (wt.%)	13.3	0.6	–
SiO_2 (wt.%)	46.8	0.02	–
Al_2O_3 (wt.%)	36.6	Min. 98.0	–
Fe_2O_3 (wt.%)	1.05	0.007	–
TiO_2 (wt.%)	0.3	0.01	–
CaO (wt.%)	0.4	–	–
MgO (wt.%)	0.3	–	–
Na_2O (wt.%)	0.03	0.15	–
K_2O (wt.%)	1.2	0.15	–
Kaolinite (wt.%)	88	–	–
Quartz (wt.%)	3	–	–
Micaceous minerals (wt.%)	9	–	–
α-Alumina (wt.%)	–	25	–

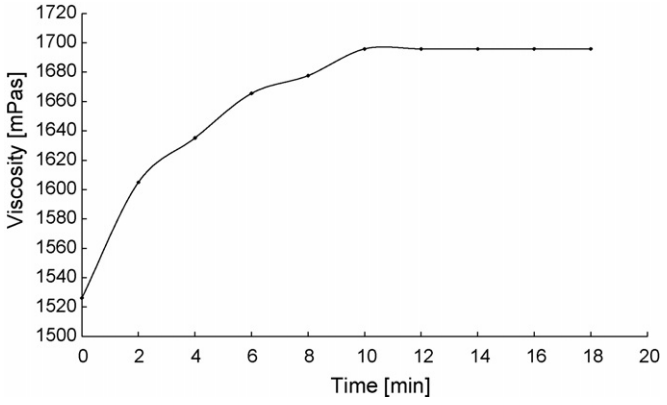

Fig. 1. Thixotropy of the kaolin–alumina suspension after shearing at 1.5 s^{-1}.

was mixed properly and poured into a mould. All prepared compositions are shown in Table 2.

The pore formation process observably starts after approximately 20 min and proceeded over a period of 45–60 min whereby volume increases up to 100–150%. Rheological measurements (Rheomat 115, Contraves, GER) were done to point out the thixotropic behaviour of the kaoline–alumina suspension (Fig. 1). Beside thixotropy the increasing viscosity due to pore formation caused stabilization of the structure.

After drying at 60–80 °C the porous body was sintered at temperatures between 1200 and 1700 °C. The bulk density of the samples was measured by the water suspension method using Archimedes' principle. Two different methods were used to analyse the pore structure. First a two-dimensional picture capture taken by a CCD-camera of each prepared sample (003, 005, 008, 010, 015) was analysed by Imaging methods (Image C, Imtronic GmbH, Berlin, GER) to get an overview about shape and size of existing pores. Time-consuming X-ray tomography (μCT 40, Scanco Medical GmbH, Bassersdorf, CH) was performed for the two selected samples 008 and 010. Using the data form X-ray tomography the computed structure model index (SMI) makes it possible to quantify the characteristic form of a three-dimensionally described structure in terms of the amount of plates and rods composing the structure. The SMI is calculated by means of three-dimensional image analysis based on a differential analysis of the triangulated foam surface. For an ideal plate and rod structure the SMI value is 0 and 3, respectively, independent of the physical dimensions. For a structure with both plates and rods of equal thickness the value lies between 0 and 3, depending on the volume ratio of rods and plates. For ideal spheres, the value equals 4. Samples with the same volume density but varying trabecular architecture can uniquely be characterized with the SMI.[16]

To identify possible variations in the batch 008 and 010 samples were prepared in foaming direction and perpendicular. Mercury porosimetry was carried out with the Pascal 140 Series (Thermal Electron Corporation, NY, USA) to detect the porosity of the cell walls, which could be neither detected with imaging methods nor with X-ray tomography in the chosen setup. The DTA-DTG analyses of the materials were carried out with the derivatograph system Paulik. The morphology of phases and the microstructure were studied by the SEM Microscope Quanta 200 (FEI Company, Hillsboro, USA) with EDAX System for the analyses of energy dispersed X-rays. X-ray diffraction patterns (PHILIPS PW 1790) were recorded after thermal treatment to evidence phase formation.

3. Results and discussion

The presented pore formation process of kaoline suspensions with metal powders is based on the aerated concrete technology using Al powders or pastes. Experimental results from former investigations show that some surfactant phyllosilicates of the kaolinite group as well as some oxides like Al_2O_3 create foams by the formation of H_2 gas from the dissolution of aluminium in alkali free water based suspensions at pH 7–9.

R. Nüesch and D.D. Eberl showed that a dilute suspension of nano minerals may catalyze the hydrolytic dissolution of Al alloy metal by water at a nearly neutral pH. The reaction is not affected

Table 2
Batch compositions

Sample	003	005	008	010	015
Kaolins (wt.%)	22.2	22.2	22.2	22.2	22.2
Alumina (wt.%)	44.4	44.4	44.4	44.4	44.4
H_2O (wt.%)	33.3	33.3	33.3	33.3	33.3
Aluminium (wt.% dry weight based)	0.03	0.05	0.08	0.10	0.15
Porosity after sintering (1500 °C) (vol.%)	67	72	73	77	79

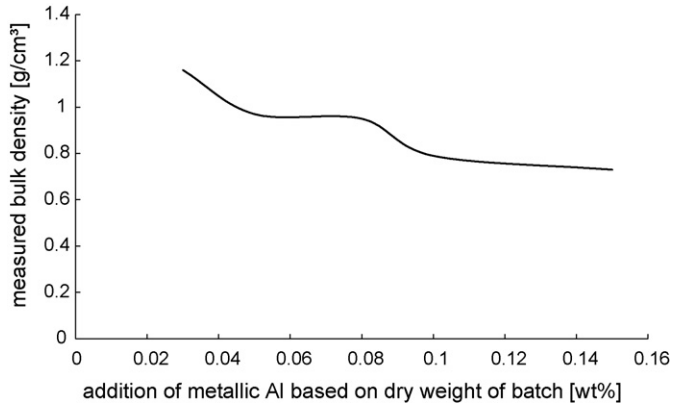

Fig. 2. Bulk densities in dependence of the added metallic precursor, samples sintered at 1500 °C.

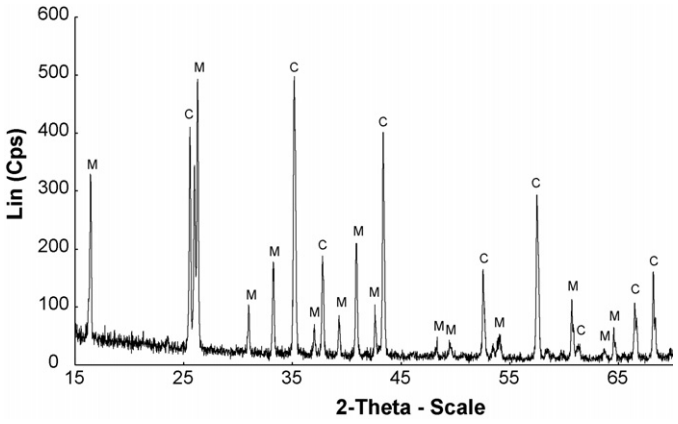

Fig. 3. XRD-pattern to demonstrate phase evolution of mullite and corundum. C: Corundum, M: mullite.

by the type of aluminium alloy used. It is promoted by different types of clay minerals and fine grained quartz, but not by Al-hydroxides. The reaction occurs, even if clays are suspended in distilled water, tap water or 1 M NaCl solutions. Nüesch and Eberl proposed a hydrolysis reaction in which clay minerals are in close contact with the Al alloy surface. The clay mineral surface properties favour proton reactions with the protective aluminiumoxide/hydroxide layer and prevent the self-healing process of the oxide layer. The on-going hydrolytic reaction of water with aluminium is promoted. Certain nano minerals serve as a semi-permeable membrane. Water is allowed to diffuse to the nano mineral metal interface where hydrolysis of the Al alloy metal takes place.[17]

It is possible to influence the pore forming reaction by the addition of organic substances like KM 1001 or KM 1002 (Zschimmer and Schwarz, Lahnstein, Germany). KM 1001 is a synthetic polyelectrolyt (density = 1.1 g/cm^3, pH 7.8 for the liquid, pH 8.5 for 0.1 wt.% solution in H_2O) which is used for dispersion and deflocculation of metal powders in water. KM 1002 (density = 1.2 g/cm^3, pH 7.1 for the liquid and 0.1 wt.% solution in H_2O) is a carboxylic acid which is also used for dispersion and deflocculation of metal powders in water. Both products make suspensions possible with high solid loadings. For the presented batch compositions both additives give positive results. Aluminium can be dispersed properly in the slurry (using KM 1001 or KM 1002) and the raising process becomes more uniform (using KM 1002). KM 1002 dispersed in the batch also shows the highest pH.

The pore formation kinetics are determined by the grain size distribution and the specific composition of metal pastes or powders (corporate secret of Schlenk Metallpulver) and by

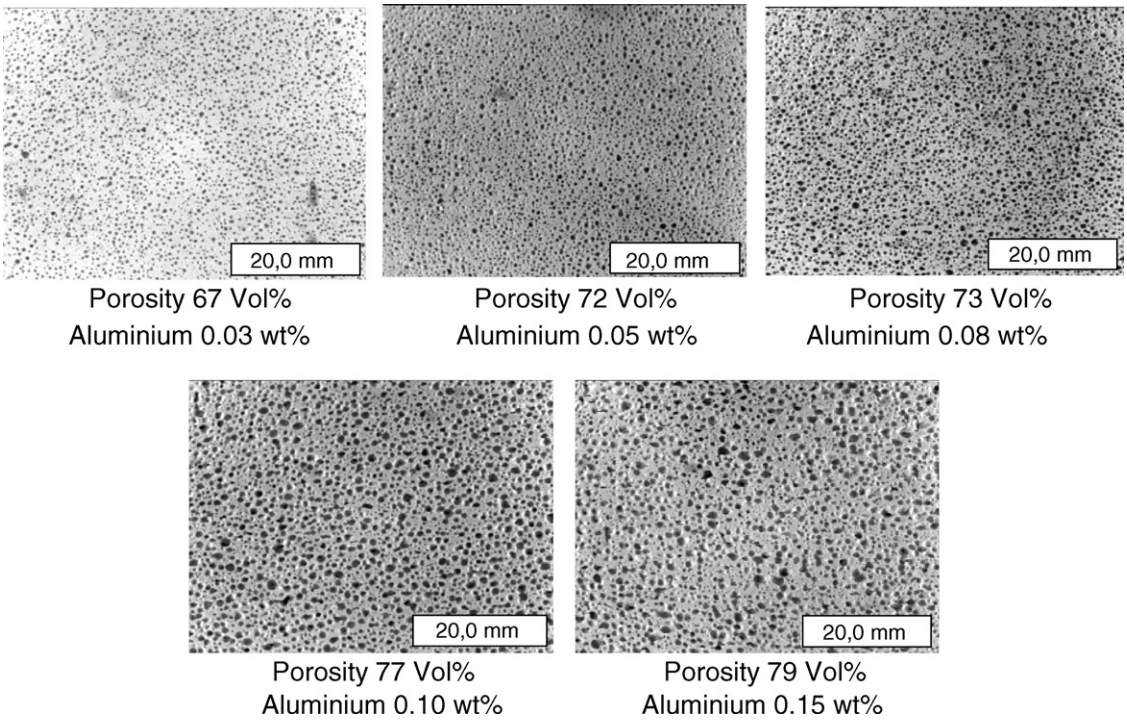

Fig. 4. Two-dimensional photo-shootings of the machined surface for IMAGE C analysis, samples sintered at 1500 °C.

Table 3
Results of image analysis

Sample	Shape factor	Convexity	Ratio of minor and major axis	Diameter area (μm)	Diameter perimeter (μm)
Green body					
003	0.76	0.96	0.71	468.03	578.45
005	0.69	0.92	0.67	537.16	888.37
008	0.68	0.91	0.67	627.1	1091.77
010	0.79	0.98	0.69	569.98	670.66
015	0.69	0.92	0.65	705.08	1151.58
Sintered body					
003	0.83	0.99	0.75	368.31	412.22
005	0.79	0.98	0.71	384.64	447.18
008	0.78	0.97	0.72	429.88	509.66
010	0.79	0.97	0.73	521.29	620.88
015	0.77	0.97	0.71	520.78	629.06

Table 4
Data from X-ray tomography of fired samples

Labelling	Series 008	Series 008 perpendicular	Series 010	Series 010 perpendicular
Bulk density (g/cm^3)	0.95	0.95	0.79	0.79
Density of connectivity (1/mm^3)	7.9427	7.4094	7.1869	6.4347
Structure model index	−1.6492	−1.6224	−0.1483	−1.6102
Relative density	0.5111	0.5093	0.3535	0.4332
Degree of anisotropy	1.1865	1.1988	1.2525	1.2269
Medium cell size (μm)	444	444	222/925	222/814
Medium cell wall size (μm)	296	296	259	296

temperature of the slurry. Small Al particles and an increased temperature accelerate the release of hydrogen and the pore formation is terminated earlier. The process allows a modification of the suspensions with specific fillers like aluminas or dead-burned fireclays up to 80 wt.% dry.

The medium pore diameter and the pore size distribution of the final product was found to be fully reproducible.

As a first approximation, bulk densities depend on the amount of added metal precursor (Fig. 2). The graph shows two levels, starting at 0.05 wt.% Al-addition and 0.1 wt.%, respectively which cause porosities of 72 and 77 vol.%. Producible porosities lie in between 67 and 79 vol.%. Adding more than 0.15 wt.% of metallic precursor is not indicated due to the formation of large instable pores.

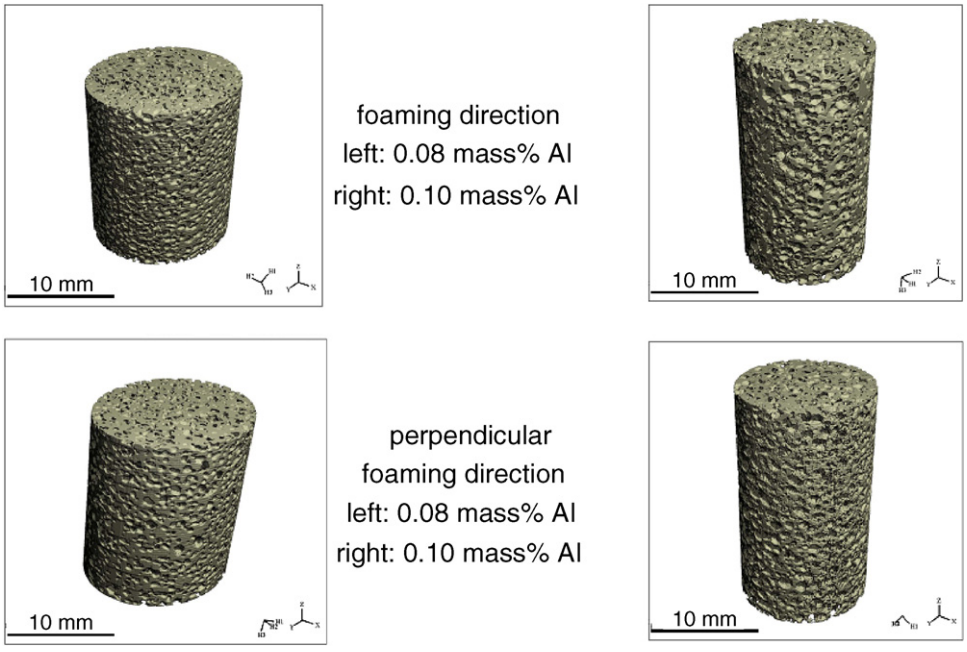

Fig. 5. Results from three-dimensional X-ray tomography measured in foaming direction and perpendicular, sample sintered at 1500 °C.

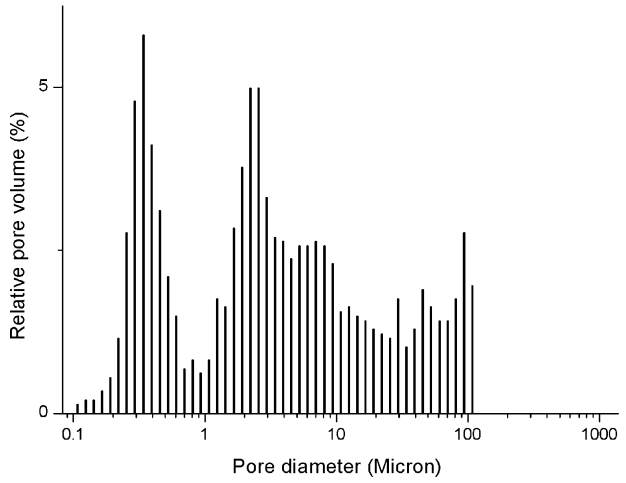

Fig. 6. Pore size distribution mercury porosimetry of the cell walls, sample 008.

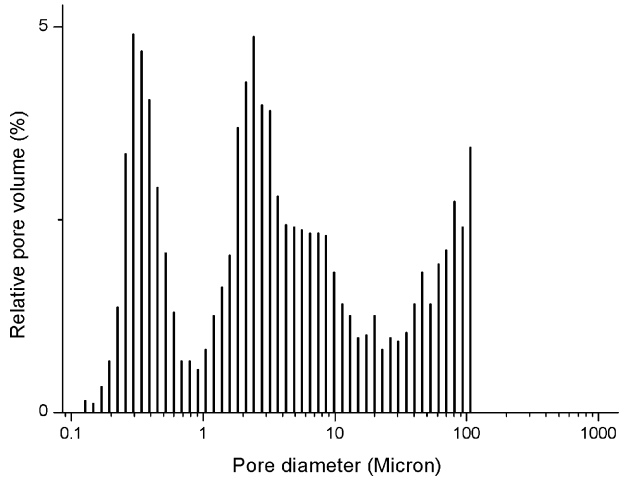

Fig. 7. Pore size distribution mercury porosimetry of the cell walls, sample 010.

Fig. 3 shows the X-ray diffraction pattern of sample 008. The observed phases are Mullite (53.5 wt.%) and Corundum (46.5 wt.%). The chemical analysis leads to 83 wt.% Al_2O_3, 16.5 wt.% SiO_2 and some minor impurities.

Fig. 4 shows two-dimensional photo-shootings of the pore structure of the investigated samples, which were used for IMAGE C analysis. The characterising parameters for the analysis are shape factor, convexity, ratio of minor and major axis, diameter area and diameter perimeter. The summary of the results is presented in Table 3. A perfect circle has a shape factor of one and the ratio of minor and major axis also equals one. The investigated materials consist all of elliptical pores with increasing pore sizes depending on increasing porosities. The differences between green body and sintered body are obvious, a shrinkage of pore size generated by the sintering process is clearly detectable. The results of X-ray tomography are shown in Fig. 5 and Table 4. The cell walls are concave as indicated by the negative structure model index values. The density of connectivity decreases with diminishing relative density. The samples of series 010 show a bimodal distribution of medium cell size indicated by the two values in medium cell size of sample series 010 in Table 4.

Both analysing methods (2-dim IMAGE C, 3-dim X-ray tomography) lead to the same results. The structure consists of elliptical pores with pore sizes depending on the adjusted porosity.

To get an idea about the existing porosity of the cell walls, which are about 300 μm thick (see Table 4), mercury porosimetry leads to the presented results (Figs. 6 and 7). Both samples (008, 010) sintered at 1500 °C show nearly the same bimodal distribution of pores less than 10 μm (pore sizes 0.3–0.4 and 2.5 μm), which can be found in the spaces between mullite needles and alumina grains (see Figs. 9–11).

The DTA-DTG of the porous, dry and unfired composites (see Fig. 8) show endothermic effects in the temperature range 260–500 °C concerned with dehydroxylation of $Al(OH)_3$

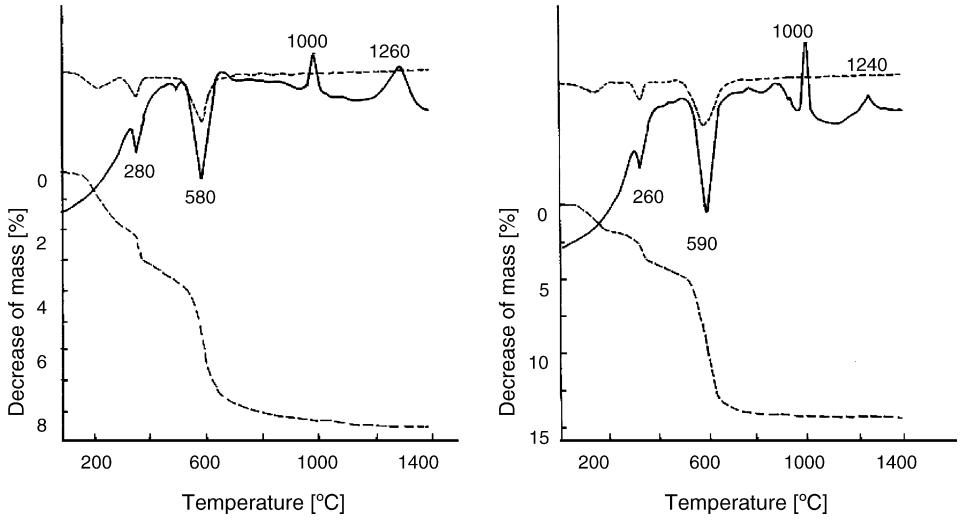

Fig. 8. DTA-DTG measurements of composite materials with Al precursor left plot: batch composition kaoline:alumina 1:2; 0.15 wt.% aluminium; 0.1 wt.% KM 1001; unfired sample right plot: batch composition kaoline:alumina 1:1; 0.15 wt.% aluminium; 0.1 wt.% KM 1001, unfired sample.

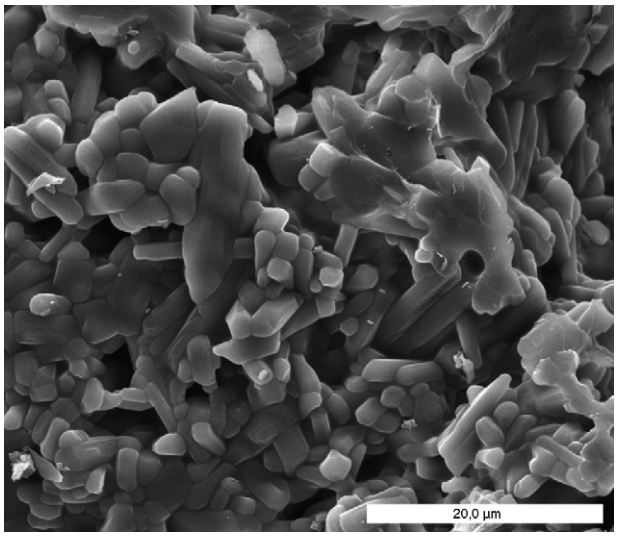

Fig. 9. SEM-micrograph sample 2 (composition "005", sintered at 1700 °C).

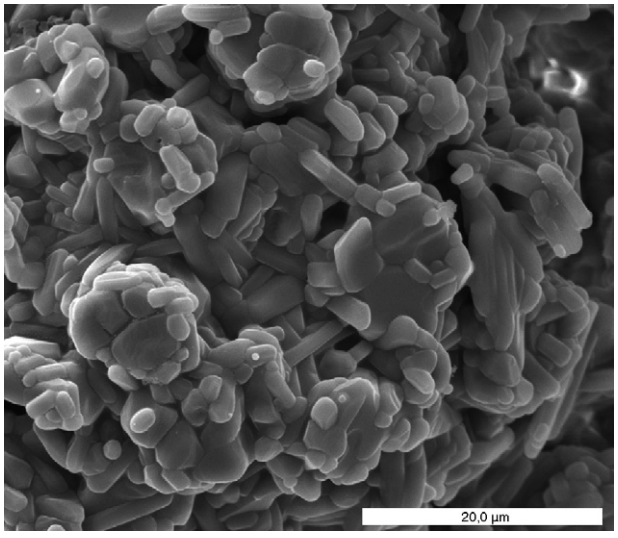

Fig. 10. SEM-micrograph sample 3 (composition "008", sintered at 1700 °C).

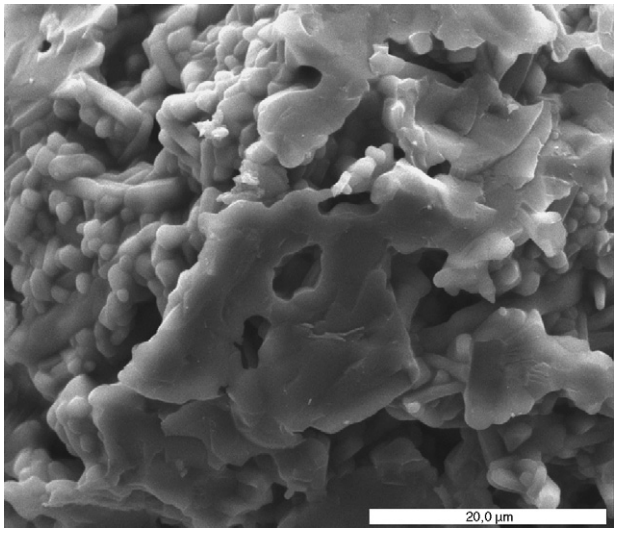

Fig. 11. SEM-micrograph "reference sample 1" (sintered at 1700 °C), kaoline: Al_20_3 = 2:1, content Al = 0.8 wt.%, content KM 1001 = 0.1 wt.%.

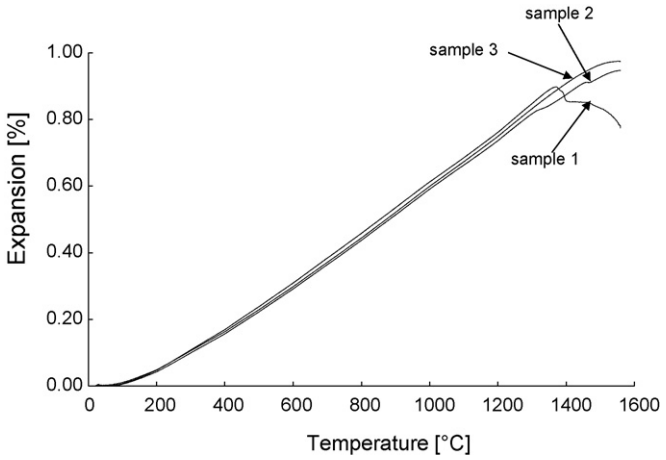

Fig. 12. Dilatometric behaviour of sample 1, 2 and sample.

formed by reaction of Al in the suspension

$$Al(OH)_3 \rightarrow AlO(OH) + H_2O \quad (100–150\,^\circ C),$$

$$2AlO(OH) \rightarrow \text{transition-}Al_2O_3 + H_2O \quad (260–500\,^\circ C)$$

At the temperature 560 °C the dehydroxylation of kaolinite starts. In comparison to the pure kaolinite the formation of spinel is shifted from about 980 °C to a temperature of about 1000 °C. The formation of mullite by higher content of alumina is shifted to higher temperatures.

Figs. 9 and 10 show the preferred microstructure for high temperature applications. Alumina grains which are wedged by well formed mullite needles could be observed in the material fired at 1700 °C (samples 2, 3) and both samples did not show any softening up to a temperature of 1550 °C in the dilatometric investigation (Fig. 12). Fig. 11 shows a reference sample (=sample 1) which still contains a considerable amount of glassy phase with embedded mullite needles which leads to softening of the material at lower temperatures (see Fig. 12).

4. Conclusions

Production of light weight refractories according to aerated concrete technology was investigated. The porosity could be varied by different amounts of metal precursor. The sintered material consists of well shaped elliptical pores with pore sizes of about 200–900 µm depending on the Al paste content. Alumina grains wedged by mullite needles could be obtained by raw materials containing only a small amount of free quartz whereupon high sintering temperatures above 1650 °C are required. The samples meet the ASTM requirements for application temperatures up to 1550 °C.

Acknowledgements

All authors would like to thank the Bavarian Science Foundation (AZ 496/02) for supporting the research activities.

References

1. Gibson, L. J. and Ashby, M. F, Cellular solids. *Structure and properties*, 2nd ed., Cambridge Solid State Series, Cambridge University Press, Cambridge, 1997.
2. Sepulveda, P. and Binner, J. G. P., Processing of cellular ceramics by foaming and in situ polymerisation of organic monomers. *J. Eur. Cer. Soc.*, 1999, **19**, 2059–2066.
3. Saggio-Woyanski, J., Scott, C. E. and Minnear, W. P., Processing of porous ceramics. *Am. Cer. Soc. Bull.*, 1992, **71**, 1674–1682.
4. Svinka, V., Moertel, H. and Krebs, S., Novel light weight refractory bricks. In Proceedings of CIMTEC 2002, 10th International Ceramic Congress, *vol. 35*, Florency, Italy, 14–18 July, 2002, pp. 149–160.
5. Jüttner, Th., Mörtel, H., Svinka, V. and Krebs, St., Novel light weight refractories for high temperature application in ceramics industry, In Procceedings of the 46th International Colloquium on Refractories, 12–13 November 2003 Aachen, Stahl und Eisen Special, 2003, pp. 154–158.
6. Pascal, J. and Zapatero, J., Preparation of mullite ceramics from coprecipitated aluminium hydroxide and kaolinite using hexamethylenediamine. *J. Am. Ceram. Soc.*, 2000, **83**, 2677–2680.
7. Katsuki, H., Furuta, S., Ichinose, H. and Nakao, H., Preparation and some properties of porous ceramic sheet composed of needle-like mullite. *J. Ceram. Soc. Jpn.*, 1988, **96**(11), 1081–1086.
8. Katsuki, H., Furuta, S. and Komarneni, S., Formation of novel ZMS-5 porous composite from sintered kaoline honeycomb by hydrothermal reaction. *J. Am. Ceram. Soc.*, 2000, **83**, 1093–1097.
9. Aksay, I. A., Dabbs, D. M. and Sarikaja, M., Mullite for structural electronic and optical application. *J. Am. Ceram. Soc.*, 1991, **74**, 2343–2357.
10. Paiva, A. M., Sepulveda, P. and Pandolfelli, V. C., Processing and thermomechanical evaluation of fibre-reinforced alumina filters. *J. Mater. Sci.*, 1999, **34**, 2641–2649.
11. Davis, R. F. and Pask, J. A., In *Part 4, Mullite in High Temperature Oxides*, ed. A. Alper. Academic Press, New York, 1971.
12. Brindley, G. M. and Nakahira, M., The kaolinite–mullite reaction series I–III. *J. Am.Ceram. Soc.*, 1959, **42**(7), 311–324.
13. Sonyparlak, B., Sarikaya, M. and Aksay, I. A., Spinel-phase formation during 980° exothermic reaction in the kaolinite-to-mullite reaction series. *J. Am. Ceram. Soc.*, 1990, **70**(11), 837–842.
14. Johnson, M., Pask, J. A. and Moya, J. S., Influence of impurities on high-temperature reactions of kaolinite. *J. Am. Ceram. Soc.*, 1982, **65**(1), 31.
15. Liu, K. C., Zhomas, G., Caballero, A., Moya, J. S. and de Aza, S., Mullite formation in kaolinite-Al_2O_3. *Acta Metall. Mater.*, 1994, **42**(2), 489–495.
16. Hildebrand, T. and Rüegsegger, P., Structure model index—a new model to describe remodelling of trabecular bone. *Bone*, 1996, **19**, Supplement 143S[75].
17. Nüesch, R. and Eberl, D. D., Nano minerals induced aluminium corrosion. *Berichte der Deutschen Mineralogischen Gesellschaft, Beihefte zum, Eur. J. Mineral.*, 2004, **16**, 1, DMG 2004 Tagung, Karlsruhe, 19–22 September 2004.